Low-Energy Charge-Density Excitations in MgB$_2$: Striking Interplay between Single-Particle and Collective Behavior for Large Momenta

Y. Q. Cai,[1, *] P. C. Chow,[1, †] O. D. Restrepo,[2, 3] Y. Takano,[4] K. Togano,[4] H. Kito,[5] H. Ishii,[1] C. C. Chen,[1] K. S. Liang,[1] C. T. Chen,[1] S. Tsuda,[6] S. Shin,[6, 7] C. C. Kao,[8] W. Ku,[9] and A. G. Eguiluz[2, 3]

[1]*National Synchrotron Radiation Research Center, Hsinchu 30076, Taiwan*
[2]*Department of Physics and Astronomy, The University of Tennessee, Knoxville, Tennessee 37996-1200, USA*
[3]*Materials Science and Technology Division, Oak Ridge National Laboratory, Oak Ridge, Tennessee 37831-6030, USA*
[4]*National Institute for Materials Science, 1-2-1 Sengen, Tsukuba 305-0047, Japan*
[5]*National Institute of Advanced Industrial Science and Technology, 1-1-4 Umezono, Tsukuba 305-8586, Japan*
[6]*Institute for Solid State Physics, University of Tokyo, Kashiwa, Chiba 277-8581, Japan*
[7]*Institute of Physical and Chemical Research (RIKEN), Sayo-gun, Hyogo 679-5198, Japan*
[8]*National Synchrotron Light Source, Brookhaven National Laboratory, Upton, NY 11973-5000, USA*
[9]*Department of Physics, Brookhaven National Laboratory, Upton, NY 11973-5000, USA*
(Dated: February 4, 2008)

A sharp feature in the charge-density excitation spectra of single-crystal MgB$_2$, displaying a remarkable cosine-like, periodic energy dispersion with momentum transfer (q) along the c^*-axis, has been observed for the first time by high-resolution non-resonant inelastic x-ray scattering (NIXS). Time-dependent density-functional theory calculations show that the physics underlying the NIXS data is strong coupling between single-particle and collective degrees of freedom, mediated by large crystal local-field effects. As a result, the small-q collective mode residing in the single-particle excitation gap of the B π bands reappears periodically in higher Brillouin zones. The NIXS data thus embody a novel signature of the layered electronic structure of MgB$_2$.

PACS numbers: 71.45.Gm, 73.43.Lp, 74.70.Ad, 78.90.+t

The discovery of superconductivity in MgB$_2$ at a high critical temperature $T_c \sim 39$ K [1] has stimulated numerous theoretical and experimental studies worldwide. Unlike high-T_c cuprates, the relatively simple crystal structure of MgB$_2$ allows detailed first-principles calculations to be performed and compared with experiments. As a result, MgB$_2$ is now widely accepted as a phonon-mediated conventional superconductor based on the anisotropic Eliashberg formalism with multiple gaps facilitated by the different electron-phonon coupling strengths of the boron σ and π bands [2, 3, 4, 5, 6, 7]. The strong electron-phonon coupling between the 2D σ bands and the in-plane vibration of the B layers (the E_{2g} phonons) dominates the superconducting properties and is largely responsible for the unusually high T_c.

Within this phonon-mediated picture of superconductivity, dynamically screened electron-electron and electron-ion interactions play an important role [8]. The study of charge-density response function through inelastic x-ray [9] or electron [10] scattering experiments and/or theoretical calculations provides a powerful means for investigating the details of the dielectric screening and the associated crystal potential, local-field, and exchange-correlation effects. Recent first-principles calculations [11, 12], for example, have shown the importance of the crystal local-field effects (CLFE) in shaping the superconducting properties of MgB$_2$. Earlier theoretical studies of the collective charge excitations in MgB$_2$ based on first-principles calculations by Ku *et al.* [13] and Zhukov *et al.* [14], on the other hand, predicted a sharp new collective mode between 2-5 eV for momentum

transfer $q\|c^*$-axis as a result of coherent charge fluctuations between the Mg and B layers due to the unique electronic structure of MgB$_2$. The feature as predicted dispersed weakly with q and decayed via Landau damping into the single-particle continuum at $q \sim 6$ nm^{-1} in the first Brillouin zone (BZ). The CLFE were reported to be negligible, for the small q-range investigated.

In this Letter we demonstrate, using state-of-the-art high-resolution non-resonant inelastic x-ray scattering (NIXS) experiments and *ab initio* time-dependent density functional theory (TDDFT) calculations, that the charge response of MgB$_2$ is truly remarkable. Indeed, the long-lived, low-energy collective excitation in MgB$_2$ exists not only for small q as previously predicted [13, 14], but it actually extends to higher BZ's along the c^*-axis. The mechanism behind such physics is the strong coupling between the single-particle and collective excitation channels which is mediated by large crystal local-field effects (CLFE) due to charge inhomogeneity normal to the Mg and B layers. As a result, the conventional Landau-damping mechanism does not restrict the collective mode to a small fraction of the momentum space: the mode actually reappears *periodically* as q steps through successive BZ's. The enhanced scattering cross section at high q and the negligible multiple-scattering effects of the x-ray measurements play a decisive role for the clean observation of this mode over a large momentum range. Our work represents also the first observation of collective charge excitations of this kind in condensed matter physics [15].

The MgB$_2$ single crystals were prepared by high-pressure sintering of MgB$_2$ powder [18]. Superconduct-

ing transition with the onset temperature of 39 K was confirmed by both magnetic and resistive measurements. The crystals were plate-like, golden in color, and measured $\sim 500 \times 300 \times 20$ μm^3 in size. The crystal quality and orientation were characterized by Laue and indexing rotation photos, in which well-defined principal Bragg diffraction spots were identified and used to align the c^*- and a^*-axis to the scattering plane. Crystals chosen for the measurement showed rocking curve widths of $\sim 0.05°$ for low order reflections. Beam damages to the crystals were not visible upon visual inspection using a microscope before and after the measurements.

NIXS spectra were collected at room temperature on the Taiwan inelastic x-ray scattering beamline BL12XU at SPring-8 [19]. The energy transfer was varied by scanning the incident energy relative to the near backscattering energy (9.886 keV) of a 2-m radius Si(555) spherical analyzer [20]. The total energy resolution was 65 and 250 meV respectively using two configurations of the beamline and the spectrometer [19]. The momentum resolution was 0.6 nm^{-1} in the horizontal scattering plane, and 2.3 nm^{-1} in the vertical plane.

Figure 1 shows a selection of the NIXS spectra taken over the energy region of the low-energy collective mode with momentum transfer q covering four entire BZ's along the c^*-axis. All spectra are raw data normalized to the incident beam intensity in unit of counts per minute. The periodic nature of this mode in energy is apparent: The feature starts at ~ 3 eV at $q = 3.0$ nm^{-1} [Fig. 1(a)], disperses down to ~ 4.5 eV at the first zone boundary at 8.9 nm^{-1} where the dispersion turns negative until it reaches near the next zone center at 17.8 nm^{-1}, and then repeats itself in the third and the fourth BZ [Fig. 1(b)]. The width of the loss feature varies also periodically, with
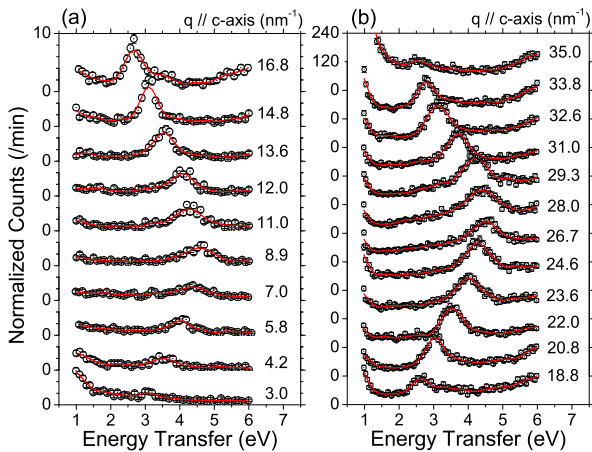
about 0.5-eV (1-eV) width at half maximum near the zone centers (boundaries). Experimentally, the energy dispersion of this mode with momentum transfer can be described entirely by a simple cosine function (see Fig. 2): $\omega = \omega_0 - 2\gamma\cos(qc)$, with $\omega_0 = 3.55$ eV, $\gamma = 0.49$ eV, and $c = 0.352$ nm the lattice constant of MgB$_2$ along the c-axis. An extrapolated value of 2.57 eV at $q = 0$ can thus be obtained, which is in excellent agreement with recent optical studies [21] and provides additional support for the experimental confirmation of this collective mode at low q.

In order to understand the physics behind the data presented in Fig. 1, we have calculated the dynamical structure factor $S(\mathbf{q}, \omega)$ based on time-dependent density functional theory (TDDFT) [22], including fully the CLFE. Being a quantity directly proportional to the scattering cross section of NIXS [9], the dynamical structure factor $S(\mathbf{q}, \omega)$ is related to the density-response function χ by the fluctuation-dissipation theorem,

$$S(\mathbf{q}, \omega) = -2\hbar V \mathrm{Im}\chi_{\mathbf{G_q}, \mathbf{G_q}}(\mathbf{q} - \mathbf{G_q}, \omega), \qquad (1)$$

where $\mathbf{G_q}$ is the unique vector of the reciprocal lattice which brings $\mathbf{q}$ into the first BZ. In TDDFT, χ obeys the formally exact integral equation $\chi = \chi_S + \chi_S(\nu + f_{XC})\chi$, where χ_S is the response function for Kohn-Sham electron-hole pairs, ν the Coulomb interaction, and f_{XC} the many-body kernel [22]. χ_S is evaluated for a ground state obtained in the local-density approximation (LDA) using the LAPW method [23]. The many-body kernel f_{XC} is evaluated for the adiabatic extension of the LDA [24], defining the TDLDA response, which in view of our NIXS data, is an excellent approximation [25]. The integral equation is then solved for the response matrix $\chi_{\mathbf{G}, \mathbf{G'}}(\mathbf{q} - \mathbf{G_q}, \omega)$ [26]. The calculated $S(\mathbf{q}, \omega)$, obtained using a damping parameter of 0.17 eV in the evaluation of χ_S, is compared with experiment in Figs. 2 and 3.

The calculated periodic energy dispersion of the collective mode represented by the dashed line in Fig. 2 can be seen to agree almost perfectly with experiment throughout the four BZ's investigated. In Fig. 3, the calculated $S(\mathbf{q}, \omega)$ is compared in detail with the NIXS spectra at a few selected q values of the second period. Here no attempt has been made to convert the experimental raw data onto absolute units due to insufficient data range to apply the f-sum rule [27]. The comparison is made therefore qualitatively with a constant scale factor between theory and experiment for all the q values shown. Nevertheless, the spectral behavior of the observed collective mode is reproduced very well by the calculation despite an overall underestimate of the spectral weight at the higher energy side.

Now, the density-response matrix can be expressed in terms of the inverse of the dielectric matrix as $\chi_{\mathbf{G}, \mathbf{G'}}(\mathbf{q} - \mathbf{G_q}, \omega) = \nu^{-1}(\mathbf{q} - \mathbf{G_q} + \mathbf{G})\left\{[\epsilon(\mathbf{q} - \mathbf{G_q}, \omega)]^{-1}_{\mathbf{G}, \mathbf{G'}} - \delta_{\mathbf{G}, \mathbf{G'}}\right\}$. For the latter, we

FIG. 1: NIXS spectra at various momentum transfers $q \parallel c^*$-axis showing the low-energy collective mode, where $q = 8.9$ nm^{-1} corresponds to the first boundary of the extended Brillouin zones (BZ). The total energy resolution was 65 meV for (a), and 250 meV for (b).
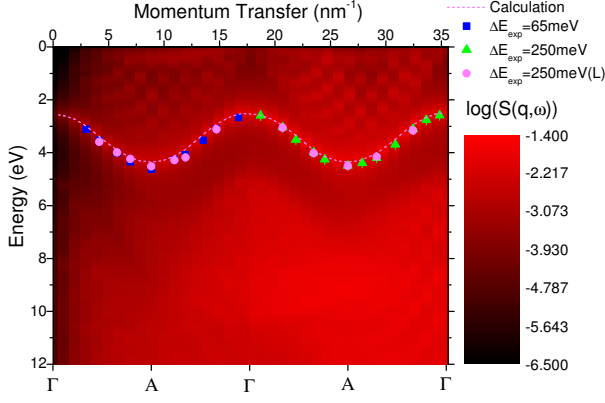
FIG. 2: (Color) Theoretical $S(\mathbf{q}, \omega)$ calculated in the present work in false color log scale as a function of energy and momentum transfer showing the cosine energy dispersion of the low-energy collective mode. Filled squares and triangles mark the energy positions obtained from the NIXS spectra shown in Fig. 1, whereas filled circles are data from another set of spectra taken with a total energy resolution of 250 meV.
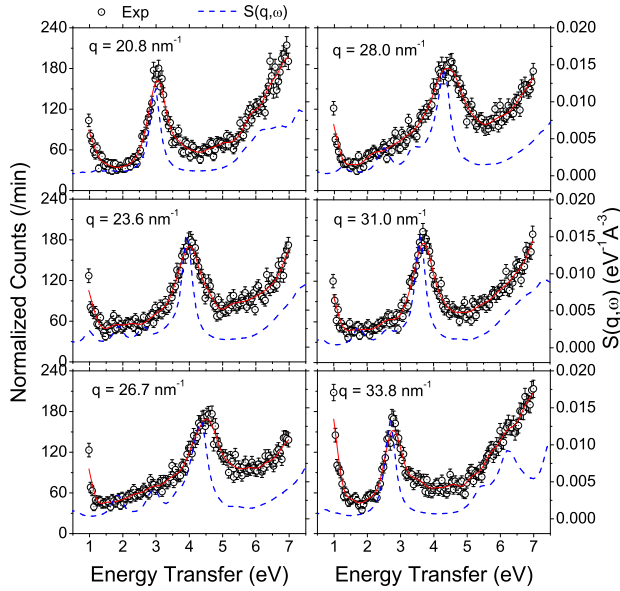

FIG. 3: Qualitative comparison between the calculated $S(\mathbf{q}, \omega)$ and the NIXS spectra at selected q values of the second period.

have derived the following exact result [28],

$$[\epsilon(\mathbf{q} - \mathbf{G_q}, \omega)]^{-1}_{\mathbf{G_q}, \mathbf{G_q}} = \frac{1}{\epsilon_{\mathbf{G_q}, \mathbf{G_q}}(\mathbf{q} - \mathbf{G_q}, \omega)}$$
$$+ F(\mathbf{q}, \mathbf{q} - \mathbf{G_q}; \omega) [\epsilon(\mathbf{q} - \mathbf{G_q}, \omega)]^{-1}_{\mathbf{0,0}} \quad (2)$$

for $\mathbf{q}$'s in higher BZ's [29]. Here $F(\mathbf{q}, \mathbf{q} - \mathbf{G_q}; \omega) = -W(\mathbf{q}, \mathbf{q} - \mathbf{G_q}; \omega)/\epsilon_{\mathbf{G_q}, \mathbf{G_q}}(\mathbf{q} - \mathbf{G_q}, \omega)$, where $W(\mathbf{q}, \mathbf{q} - \mathbf{G_q}; \omega) = \left(Det[\epsilon] - \epsilon_{\mathbf{G_q}, \mathbf{G_q}} M_{\mathbf{G_q}, \mathbf{G_q}}\right)/M_{\mathbf{0,0}}$, $M_{\mathbf{0,0}}$ and $M_{\mathbf{G_q}, \mathbf{G_q}}$ being the minor of the $(\mathbf{G} = \mathbf{0}, \mathbf{G'} = \mathbf{0})$ and

$(\mathbf{G} = \mathbf{G_q}, \mathbf{G'} = \mathbf{G_q})$ elements of ϵ, respectively. Here, the arguments of all quantities shown symbolically are $(\mathbf{q} - \mathbf{G_q}, \omega)$.

Equation (2) brings out the physics of the charge response for $\mathbf{q}$'s in higher BZ's quite vividly. The first term corresponds to the response appropriate for homogeneous media; it gives rise to charge fluctuations involving incoherent electron-hole pairs. The second term introduces all the CLFE. For $\mathbf{q} - \mathbf{G_q}$ near the zone center, collective charge fluctuations (plasmons) are built into the response function $[\epsilon(\mathbf{q} - \mathbf{G_q}, \omega)]^{-1}_{\mathbf{0,0}}$; whether such excitation is actually realized in $S(\mathbf{q}, \omega)$ (via Eq. (1)) depends on the impact of the *material-dependent* coupling function $F(\mathbf{q}, \mathbf{q} - \mathbf{G_q}, \omega)$.

In Fig. 4, the contributions to the $S(\mathbf{q}, \omega)$ of MgB_2 from the first and second terms of Eq. (2) are shown for $q = 32.7$ nm^{-1} in the fourth BZ along the c^*-axis. Clearly, in the energy region relevant for the collective mode associated with the single-particle excitation gap of the B π bands [13, 14], the first term amounts to a weak background, while the second term features a sharp peak, which is typical of $\mathbf{q} - \mathbf{G_q}$ near the zone center ($|\mathbf{q} - \mathbf{G_q}| = 2.9$ nm^{-1} in Fig. 4). Now as shown in the insert of Fig. 4, ReF is *positive and nearly constant* for energies around the collective mode, while ImF goes through a local zero. Such an F ensures that the second term of Eq. (2) is controlled by Im$[\epsilon(\mathbf{q} - \mathbf{G_q}, \omega)]^{-1}_{\mathbf{0,0}}$. In other words, in MgB_2 F feeds the small-$(\mathbf{q} - \mathbf{G_q})$ physics into the charge fluctuations for large $\mathbf{q}$'s. The plasmon can be viewed as acting - via F - as a source (additional to the external field of the x-ray photon) driving a collective charge fluctuation generated in a NIXS event for large $\mathbf{q}$'s. It is important to notice that this process is intrinsically periodic. Indeed, the fact that for higher BZ's the loss feature retraces its energy dispersion in the first BZ reflects the impact on $S(\mathbf{q}, \omega)$, via the cou-
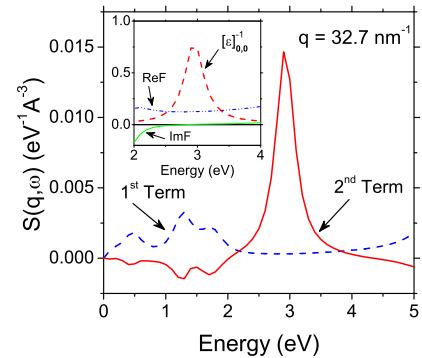

FIG. 4: Contributions calculated from the first and second terms in Eq. (2) to the $S(\mathbf{q}, \omega)$ of MgB_2 at $q = 32.7$ nm^{-1} along the c^*-axis. The insert shows the real and imaginary parts of the F factor and the $[\epsilon]^{-1}_{\mathbf{0,0}}$ for the corresponding $|\mathbf{q} - \mathbf{G_q}| = 2.9$ nm^{-1}, where $\mathbf{G_q} = (2\pi/c)(0, 0, 2)$.

pling function F in Eq. (2), of the "periodic" condition $\epsilon_{\mathbf{G},\mathbf{G}'}(\mathbf{q} - \mathbf{G_q}, \omega) = \epsilon_{\mathbf{G},\mathbf{G}'}(\mathbf{k}, \omega)$, where $\mathbf{k}$ is in the first BZ.

It is also interesting to note that there is a non-trivial difference between the response in the higher BZ's and that in the first one. In higher BZ's the collective mode arises from the "propagation" of the excitation gap of the B π bands built into $\epsilon_{\mathbf{0},\mathbf{0}}$ via the inverse dielectric matrix of the second term in Eq. (2). *This is the essence of the CLFE, in this context.* By contrast, in the first BZ the excitation gap is directly built into the scalar response $1/\epsilon_{\mathbf{0},\mathbf{0}}(\mathbf{q}, \omega)$ [29].

Additional insight into the charge response of MgB_2 is achieved in light of a simplified version of Eq. (2), corresponding to the 2×2 dielectric-matrix model invoked by Sturm, Schülke, and Schmitz [30] in their study of the $S(\mathbf{q}, \omega)$ of Si. For Si, F is complex with a *negative* real part; thus the CLFE yield only a *weak Fano-type* resonance, which highlights the novelty of the charge response of MgB_2. As we show elsewhere [28], a 2×2 dielectric-matrix model represents a fair approximation to the full calculations we have performed for MgB_2 using dielectric matrices of rank up to 23 and an $18\times18\times18$ k-mesh. (For $\mathbf{q} - \mathbf{G_q}$ near each higher BZ boundary a 3×3 model becomes necessary [28].) In such a 2×2 model, the response function from the second term of Eq. (2) becomes simply $1/\epsilon_{\mathbf{0},\mathbf{0}}(\mathbf{q} - \mathbf{G_q}, \omega)$, which makes obvious the identification of the plasmon discussed above with the collective mode discussed in Refs. [13] and [14] for $\mathbf{q}$'s near the first BZ Γ point. Most importantly, the fact that a dielectric matrix of rank two (or three) describes the response of MgB_2 rather accurately is traced to the layered structure of MgB_2, which yields a first shell of non-zero $\mathbf{G}$'s containing only two vectors, and to the fact that the length scale of the polarization in real space is determined by orbitals which are rather extended, leading to a sufficiently fast decay of $\epsilon_{\mathbf{G},\mathbf{G}'}$; therefore, increasing the rank of the ϵ-matrix beyond two or three does not affect the physics, in contrast to the case of, e.g., transition-metal oxides [28].

In conclusion, the electron-hole degrees of freedom in MgB_2 lead to a novel charge response: long-lived *collective* charge-density fluctuations can be excited in a NIXS event involving large momenta - corresponding to length scales which are comparable with the size of the B p orbitals. This is qualitatively different from the case of simple metals and covalent semiconductors discussed in Ref. [30], the difference stemming from the fact that the coupling function F is ~ 60 times larger in MgB_2. The CLFE were shown to dominate the physics of the charge excitations for large momenta, leading to the striking periodicity exhibited by the observed low-energy excitation as the momentum transfer steps through successive BZ's. Overall, the impact of the CLFE on the charge response of MgB_2 rivals their importance in materials involving confined geometries such as carbon nanotubes

[31] and superlattices [32]. Ultimately, the nature of the measured charge excitations stems from the layered electronic structure of MgB_2 and the delocalized nature of the orbitals involved in the screening. Analogous physics should be at play in other layered compounds of current interest.

---

* Electronic address: cai@nsrrc.org.tw
† Present address: HP-CAT, Advanced Photon Source, Argonne National Laboratory, Argonne, IL 60439, USA
[1] J. Nagamatsu *et al.*, Nature (London) **410**, 63 (2001).
[2] S. L. Bud'ko *et al.*, Phys. Rev. Lett. **86**, 1877 (2001).
[3] J. M. An and W. E. Pickett, Phys. Rev. Lett. **86**, 4366 (2001).
[4] J. Kortus *et al.*, Phys. Rev. Lett. **86**, 4656 (2001).
[5] A. Y. Liu, I. I. Mazin, and J. Kortus, Phys. Rev. Lett. **87**, 087005 (2001).
[6] H. J. Choi *et al.*, Phys. Rev. B **66**, 020513(R) (2002), and Nature (London) **418**, 758 (2002).
[7] S. Tsuda *et al.*, Phys. Rev. Lett. **91**, 127001 (2003).
[8] W. L. McMillan, Phys. Rev. **167**, 331 (1968).
[9] W. Schülke, J. Phys.: Condens. Matter **13**, 7557 (2001).
[10] H. Raether, *Excitation of Plasmons and Interband Transitions by Electrons* (Springer, Berlin, 1980).
[11] C.-Y. Moon, Y.-H. Kim and K. J. Chang, Phys. Rev. B **70**, 104522 (2004).
[12] A. Floris *et al.*, Phys. Rev. Lett. **94**, 037004 (2005).
[13] W. Ku, W. E. Pickett, R. T. Scalettar, and A. G. Eguiluz, Phys. Rev. Lett. **88**, 057001 (2002).
[14] V. P. Zhukov, V. M. Silkin, E. V. Chulkov, and P. M. Echenique, Phys. Rev. B **64**, 180507(R) (2001).
[15] A hint of this periodicity was contained in the NIXS data of Galambosi *et al.* [16] who reported spectra for the first two BZ's. Similarly, the work of Goldoni *et al.* [17] included a suggestion of this small-q collective mode. However, the rich physics behind the large-q NIXS data reported here was not anticipated by these works.
[16] S. Galambosi *et al.*, Phys. Rev. B **71**, 060504(R) (2005).
[17] A. Goldoni *et al.*, Phys. Rev. B **66**, 132503 (2002).
[18] Y. Takano *et al.*, Appl. Phys. Lett. **78**, 2914 (2001).
[19] Y. Q. Cai *et al.*, in *Synchrotron Radiation Instrumentation: Eighth Internationl Conference on Synchrotron Radiation Instrumentation*, AIP Conf. Proc. No. 705 (AIP, New York, 2004), p. 340.
[20] D. J. Wang *et al.*, in Ref.[19], p. 869.
[21] V. Guritanu *et al.*, Phys. Rev. B **73**, 104509 (2006).
[22] M. Petersilka, U. J. Gossmann, and E. K. U. Gross, Phys.

Rev. Lett. **76**, 1212 (1996).

[23] P. Blaha *et al.*, WIEN2k (Karlheinz Schwarz, Techn. Universität Wien, Austria), 2001.

[24] E. K. U. Gross, J. F. Dobson, and M. Petersilka, in *Density Functional Theory II*, edited by R. F. Nalewajski (Springer, Berlin, 1996), p. 81.

[25] As it turns out, in MgB_2 the many-body kernel plays a small role; in fact, even ignoring it altogether yields spectra which are in good agreement with our IXS data.

[26] I. G. Gurtubay *et al.*, Phys. Rev. B **70**, 201201(R) (2004).

[27] J. Z. Tischler *et al.*, Phys. Stat. Sol. (b) **237**, 280 (2003).

[28] O. D. Restrepo and A. G. Eguiluz, to be published.

[29] For $\mathbf{q}$'s in the first BZ, Eq. (2) becomes: $[\epsilon(\mathbf{q},\omega)]^{-1}_{\mathbf{0},\mathbf{0}} = 1/\epsilon_{\mathbf{0},\mathbf{0}}(\mathbf{q},\omega) + F(\mathbf{q},\mathbf{q}-\mathbf{G}_2;\omega)\,[\epsilon(\mathbf{q},\omega)]^{-1}_{\mathbf{G}_2,\mathbf{G}_2}$, where $\mathbf{G}_2 = (2\pi/c)(0,0,-1)$ [28]. The first term here corresponds to the response function considered in Refs. [13] and [14].

[30] K. Sturm, W. Schülke, and J. R. Schmitz, Phys. Rev. Lett. **68**, 228 (1992).

[31] A. G. Marinopoulos, L. Reining, A. Rubio, and N. Vast, Phys. Rev. Lett. **91**, 046402 (2003).

[32] S. Botti *et al.*, Phys. Rev. B **70**, 045301 (2004).